



PROJECT ACRONYM

CUPIDO

PROJECT TITLE

Cardio Ultraefficient nanoParticles for Inhalation of Drug prOducts

Deliverable 4.3

Extension of open-source flow simulation framework to also include porous media flow.

Establish relationship between different nanoparticles and deposition sites in both small and large animal models (M36)

CALL ID	H2020-NMBP-2016-2017		
GA No.	720834		
MAIN CONTACT	Kristian Valen-Sendstad Email: kvs@simula.no		
NATURE	Report (R)	DISSEMINATION LEVEL	PU
DUE DATE	31/01/2020	ACTUAL DELIVERY DATE	31/01/2020
AUTHOR(S)	Alexandra Diem, Kristian Valen Sendstad		



Table of Revisions

REVISION NO.	DATE	WORK PERFORMED	CONTRIBUTOR(S)
1	5/12/2019	Document preparation	Alexandra Diem, Kristian Valen Sendstad
2	6/12/2019	Revision	Daniele Catalucci
3	10/12/2019	Revision	CCG
4	8/01/2020	Revision	IPR Team
5	30/01/2020	Formatting	Paulina Piotrowicz



Table of Contents

1. Executive summary	5
2. Cooperation between participants	5
3. Coupling of the multi-compartment porous media model to models of cardiac contraction.....	6
3.1. Extension to a fully coupled poroelastic model.....	6
3.2. Model reduction to one-way coupling	7
3.3. Nanoparticle distribution	9
4. Conclusions	11
5. References.....	11



Index of Figures and Tables

Figure 1. Inflation of a left ventricle geometry using the fully poroelastic, two-way coupled model. Pressure is given in kPa, fluid mass is given in g	7
Figure 2. Geometry of an idealised left ventricle based on an ellipsoid used in the following simulations. The arrows indicate muscle fiber orientations used for both the contraction model, as well as the permeability tensor.	8
Figure 3. Deformation of the left ventricle during a cardiac cycle. (a) Maximum inflation at end diastole (left), and contraction at peak systole (right), scaled by a factor of two. (b) Volume change of the left ventricle.....	9
Figure 4. Myocardial perfusion pressure in an idealised left ventricle (top row, units kPa for compartment 0 and units Pa for compartments 1 and 2), and angular velocity (bottom row, units mm/s).	10
Figure 5. NP distribution as a fraction of full perfusion at $t = 0.5, 1.0, 1.5, 2.0, 2.5$ s.....	10



1. Executive summary

This deliverable extends the work described in Deliverable 4.2 and focuses on the inclusion of cardiac contraction as a driving force for the previously developed porous media flow models. We have previously demonstrated the feasibility of implementing perfusion through the myocardium using a porous media model. This model describes blood pressure through the myocardium as a result of blood flow being fed into the tissue from the surrounding arteries. Nanoparticle (NP) distribution has previously been tracked using conventional reaction-advection-diffusion (RAD) equations. In this deliverable, we have used our novel method to efficiently track NP via particle-tracking. This method has been published in the Biophysical Journal (Diem and Valen-Sendstad, Biophys J. 2019).

During the development of this deliverable some obstacles had to be overcome. Coupling of the fluid pressure to cardiac contractions into a fully poroelastic model resulted in a very stiff, and thus difficult to solve, system of equations as predicted in the risk assessment. We found that the influence of fluid pressure onto the material properties was minimal and could thus be neglected.

Key deliverable achievements:

- Coupling of cardiac contraction to porous media flow;
- Efficient implementation by model reduction;
- Tracking of NP in a heart geometry.

2. Cooperation between participants

The content of this deliverable is purely numerical based and thus did not directly involve interactions with the other project participants.



3. Coupling of the multi-compartment porous media model to models of cardiac contraction

All equations described in this deliverable are solved using the open-source finite element (FE) framework FEniCS in Python.

Previously (see D4.2) we have modelled perfusion to the heart as a multi-compartment porous media problem. This model is an adequate first order approximation but does not account for the large strains from the inflation and contraction of the heart during the cardiac cycle. In this deliverable, we thus describe the extension of this model to include cardiac contractions.

Recall from deliverable D4.2 that the multi-compartment porous media model reads

$$-\nabla \cdot (\mathbf{K}_i \cdot \nabla p_i) + \sum_{k=1}^N \beta_{i,k} (p_i - p_k) = s_i \quad (1)$$

with permeability tensors \mathbf{K}_i , pressures p_i , and inter-compartment coupling coefficients $\beta_{i,k}$ with boundary conditions

$$p_i = g_i \quad \text{on } \Gamma_N \quad (2)$$

$$-\nabla \cdot (\mathbf{K}_i \cdot \nabla p_i) \cdot \mathbf{n} = \psi_i \quad \text{on } \Gamma_D \quad (3)$$

on Neumann boundaries Γ_N and Dirichlet boundaries Γ_D , where g_i refers to a given boundary pressure, \mathbf{n} is the unit outward normal vector and ψ_i describes the normal component of a prescribed velocity on the boundary. The reduced porous media model yields pressure as a solution, while velocity can be recovered by

$$\mathbf{w}_i = -\mathbf{K}_i \cdot \nabla p_i \quad (4)$$

3.1. Extension to a fully coupled poroelastic model

The multi-compartment pure porous media model is easy to implement and solve but has severe limitations. Stress from myocardial tissue, which arguably provides the largest force to blood vessels embedded into the tissue, during the cardiac cycle is not taken into account. Cookson et al. (2012) have extended the pure porous model to a poroelastic model, where the material properties of the material are affected by the volume of fluid present, and fluid pressure is affected by stress in the tissue material. The governing equations for the fully poroelastic model are

$$\nabla_X \cdot (\mathbf{F}\mathbf{S}) = 0 \quad (5)$$

for the deformation gradient tensor \mathbf{F} and second Piola-Kirchhoff stress tensor \mathbf{S} , which is defined by the material properties Ψ_s

$$\Psi_s = a \left[\exp \left(D_1 \left(I_1 \left(1 + \sum_i^N Q_1^i \frac{m_i}{\rho} \right) - 3 \right) + D_2 \left(I_2 \left(1 + \sum_i^N Q_2^i \frac{m_i}{\rho} \right) - 3 \right) + D_3 \left((J-1)^2 + \sum_i^N Q_3^i \left(\frac{m_i}{\rho} \right)^2 \right) \right) - 1 \right] \quad (6)$$

with material specific properties a , D_1 , I_1 , Q_1 , D_2 , I_2 , Q_2 , D_3 , Q_3 such that

$$\mathbf{S} = \frac{\partial \Psi_s}{\partial \mathbf{E}} + \lambda J \mathbf{C}^{-1} \quad (7)$$

for $J = \det \mathbf{F}$ and Cauchy-Green deformation tensor $\mathbf{C} = \mathbf{F}^T \mathbf{F}$. Fluid pressure is then given by

$$p_i = \frac{\partial \Psi_s}{\partial (J \phi)} - \lambda \quad (8)$$

The equations for the fluid are solved in terms of fluid mass increase m_i



$$\frac{dm_i}{dt} = -\nabla_X \cdot (-\rho J \mathbf{F}^{-1} \mathbf{K}_i \mathbf{F}^{-T} \nabla_X p_i) + \sum_{k=1}^N -J \beta_{i,k} (p_i - p_k) + \rho q_i \quad (9)$$

Here, the first term on the right-hand side of equation (9) corresponds to the first term on the left-hand side in equation (1), taking into account material deformations during the cardiac cycle, while the last term on the right-hand side of equation (9) is equal to the second term on the left-hand side in equation (1). Fluid sources are given by the quantity q_i .

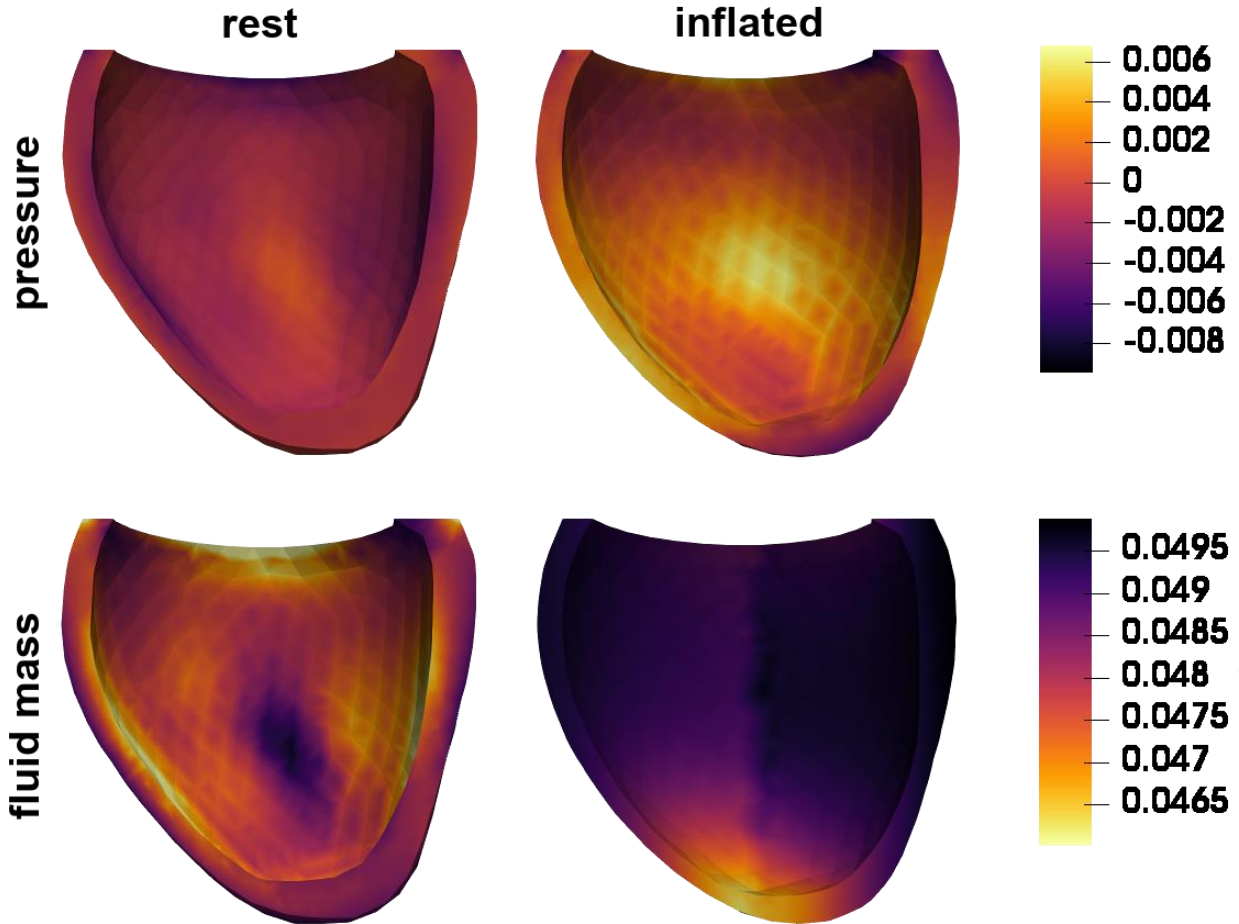


Figure 1. Inflation of a left ventricle geometry using the fully poroelastic, two-way coupled model. Pressure is given in kPa, fluid mass is given in g.

Figure 1 shows pressure and fluid mass in compartment 0 for an inflation of the fully coupled poroelastic model. We were not able to obtain results for the contraction part of the cardiac cycle due to numerical problems. The fully coupled system of equations is very stiff, and thus we could not reach convergence for the rapid increase in strain for cardiac contraction. However, the results of the inflation simulations suggested that it is reasonable to assume that the stress exerted onto the material outweighs the influence of small changes in total fluid mass onto the material properties of the tissue. To be able to solve for contraction in addition to inflation it was thus decided to remove the coupling between total fluid mass and the material properties. The resulting one-way coupled model is described in detail in the following section.

3.2. Model reduction to one-way coupling

To remove the coupling between total fluid mass and the material properties the material law Ψ_s was changed to a Holzapfel-Ogden (2009) type model that is typically used for pure solid mechanics applications, where

$$\Psi_s = \frac{a}{2b} (\exp(b(I_1 - 3)) - 1) + \frac{a_f}{2b_f} (\exp(b_f(I_{4f0} - 1))^2 - 1) \quad (10)$$



with material parameters a , b , l_1 , a_f , b_f , l_{4f0} . All other model equations remain unchanged. Additionally, the pressure term is modified to

$$p = \frac{\partial \Psi_s}{\partial \mathbf{F}} \cdot \mathbf{F}^T - \lambda \quad (11)$$

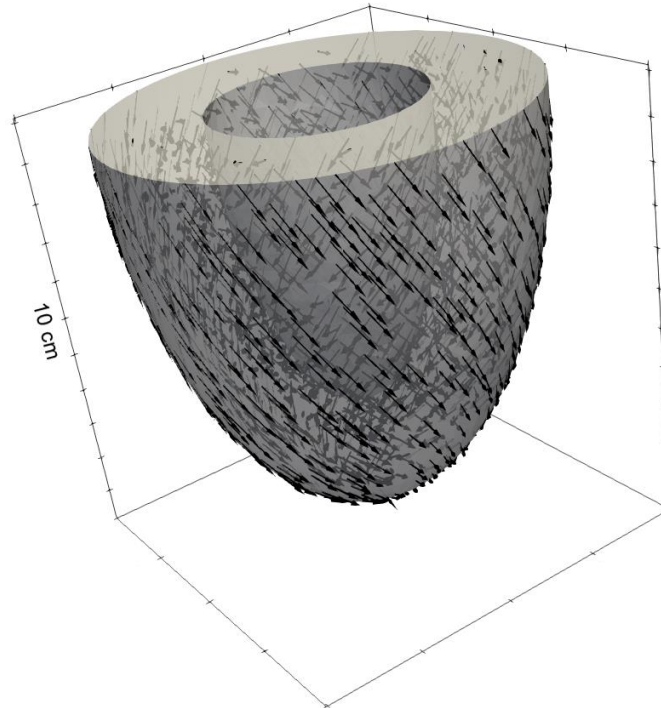


Figure 2. Geometry of an idealised left ventricle based on an ellipsoid used in the following simulations. The arrows indicate muscle fiber orientations used for both the contraction model, as well as the permeability tensor.

Implementation of active contraction requires information about the muscle fiber orientations as contraction occurs as a rapid shortening of these muscle fibers within the myocardial tissue. Muscle fibers are generally oriented helically from the base to the apex, creating the characteristic twisting of the heart during contraction. As information on the muscle fibers was not available from the patient-specific geometry we have worked with until this point, we chose to use an idealised left ventricle geometry based on an ellipsoid. By this approach it is possible to calculate fiber orientations using a rule-based approach that is based on a combination of preserving a prescribed fiber orientation angle and energy minimisation (Bayer et al. 2012, see Figure 2). Tissue contraction is then achieved by active shortening of the muscle fibers. To achieve this the deformation gradient tensor \mathbf{F} is decomposed into an elastic \mathbf{F}_e and inelastic component \mathbf{F}_a

$$\mathbf{F} = \mathbf{F}_e \mathbf{F}_a \quad (11)$$

Figure 3 shows the results of a cardiac cycle simulation using the Holzapfel-Ogden type material. To achieve inflation of the left ventricle a constant pressure of 10 kPa is applied for the duration of diastole in the left ventricle cavity. The left ventricle first expands rapidly, then more slowly as the material is stretched. Contraction is rapid and followed by a short relaxation phase bringing the geometry back to its resting state.

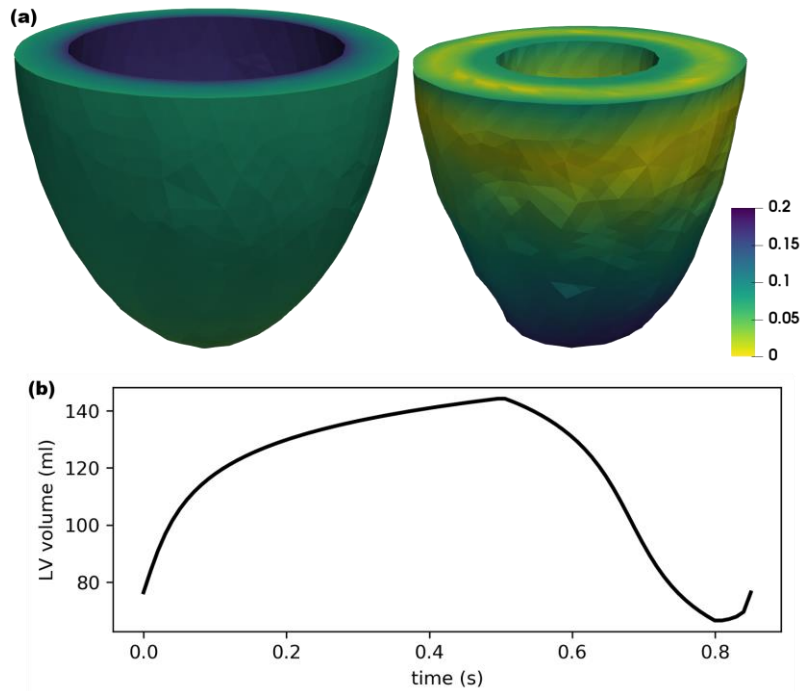


Figure 3. Deformation of the left ventricle during a cardiac cycle. (a) Maximum inflation at end diastole (left), and contraction at peak systole (right), scaled by a factor of two. (b) Volume change of the left ventricle.

Using this contraction model for a full cardiac cycle perfusion can then be evaluated using equation (9) to obtain pressure and

$$\frac{\mathbf{F}M_i}{\rho} = -\mathbf{K}_i\mathbf{F}^{-T}\nabla p_i \quad (12)$$

with

$$M_i = J\mathbf{F}^{-1}\mathbf{w}_i \quad (13)$$

to obtain velocity.

The results of this one-way coupling were presented at Computing in Cardiology 2019 and are published in the conference proceedings (Diem and Valen-Sendstad 2019a). Myocardial perfusion pressure and angular velocity are shown in Figure 4 (top and bottom row, respectively). In the large arterioles (compartment 0, left) flow is largely dominated by stress originating from tissue contraction with a range that is much larger than predicted by pure porous models (Diem and Valen-Sendstad 2019b, Michler et al. 2013). The narrow pressure ranges in small arterioles and capillaries suggest that coupling coefficients β are sensitive to the pressure range within the large arterioles, and thus differences across compartments. Velocities are given in the angular direction and are displayed on a logarithmic scale.

3.3. Nanoparticle distribution

To track NP under cardiac contraction we use our recently developed particle tracking method (Diem and Valen-Sendstad 2019b). NP distribution is shown in Figure 5. NP are injected at five locations around the heart and are not consumed by the tissue to allow for the study of distribution patterns. After three cardiac cycles ($t = 2.5$ s) the left ventricle has reached a minimum of 10% perfusion everywhere, while locations around the injection sites reach 50-90%.

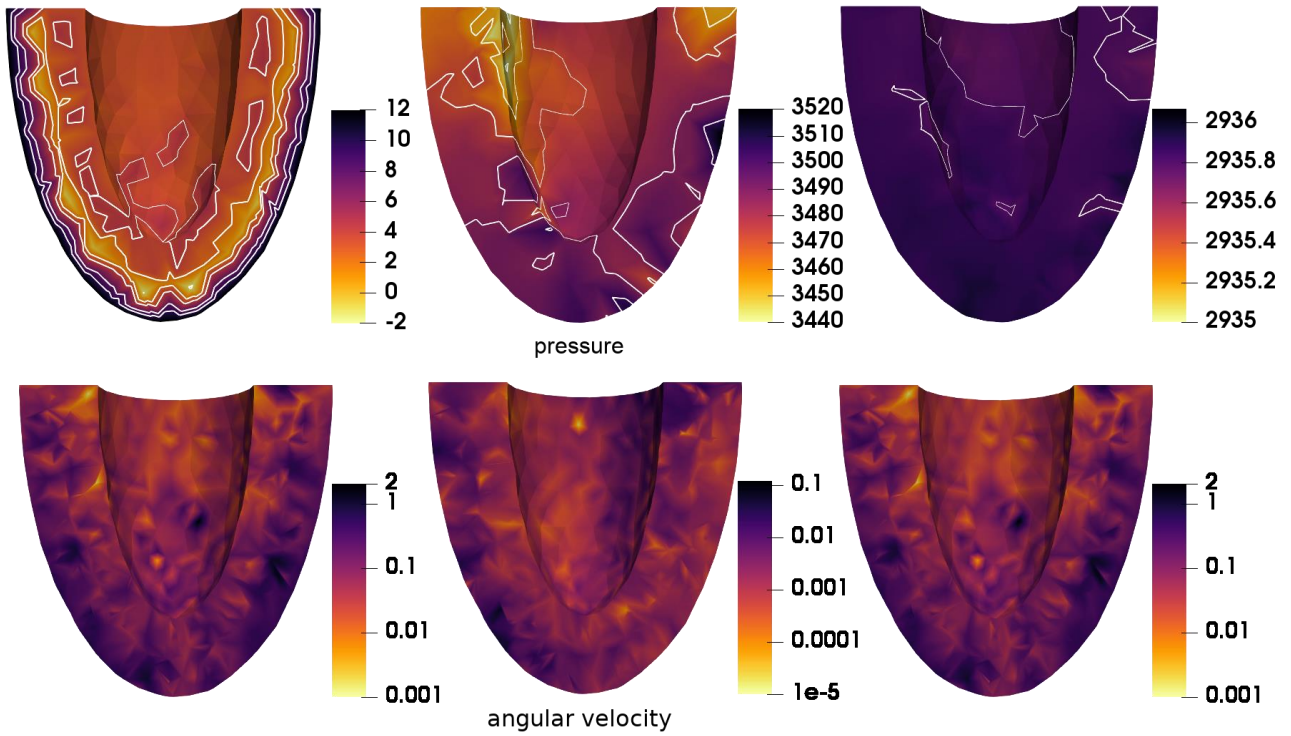


Figure 4. Myocardial perfusion pressure in an idealised left ventricle (top row, units kPa for compartment 0 and units Pa for compartments 1 and 2), and angular velocity (bottom row, units mm/s).

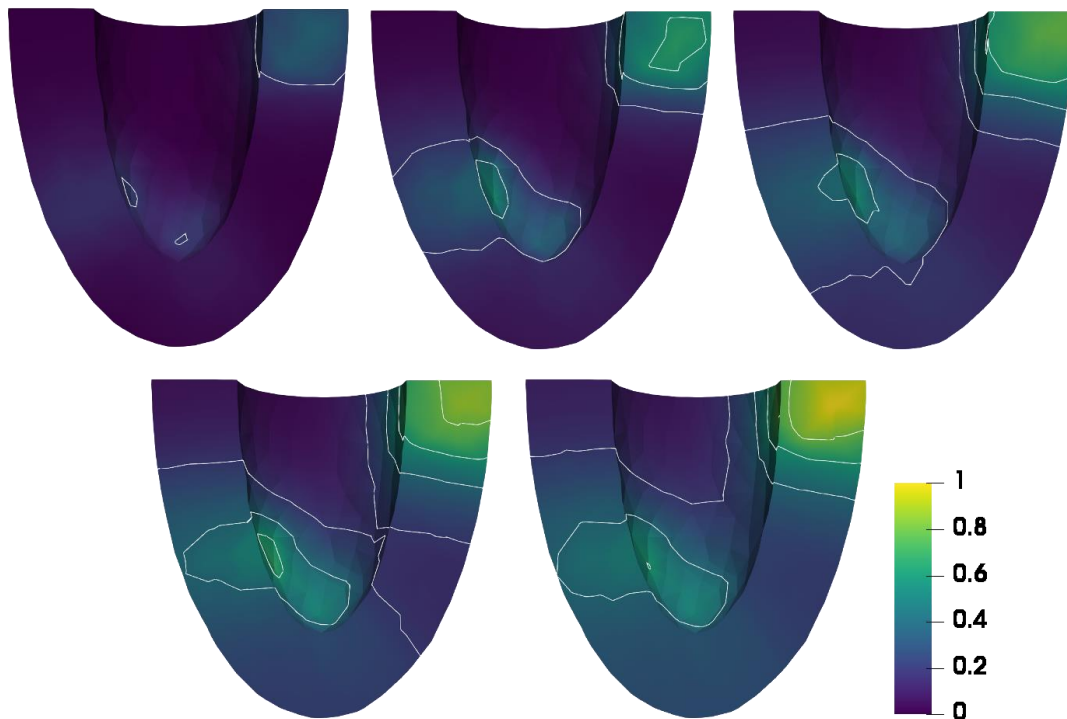


Figure 5. NP distribution as a fraction of full perfusion at t = 0.5, 1.0, 1.5, 2.0, 2.5 s.



4. Conclusions

Simulating a full cardiac cycle using a fully coupled poroelastic model has until this point not been achieved. An alternative solution was to remove the influence of the fluid mass present in the myocardial tissue on tissue stiffness and instead consider a one-way coupled model. Combining this approach with our NP tracking method, which is published in the *Biophysical Journal*, we are able to efficiently track any type of tracer distributed via perfusion.

Here, we have used this approach to demonstrate NP distribution in an idealised left ventricle geometry of a human heart. This work has been presented at Computing in Cardiology. There are some discrepancies in perfusion pressure between our mechanics driven model and pure perfusion models, indicating the sensitivity of parameters such as permeability and especially inter-compartment coupling coefficients to the mechanics. A large-scale sensitivity analysis is thus required to resolve the mechanisms behind organ perfusion and cardiac diseases that develop over large timeframes, such as heart failure due to myocardial remodelling.

5. References

1. Bayer, J. D., Blake, R. C., Plank, G., & Trayanova, N. A. (2012). A novel rule-based algorithm for assigning myocardial fiber orientation to computational heart models. *Annals of Biomedical Engineering*, 40(10), 2243–2254. <https://doi.org/10.1007/s10439-012-0593-5>
2. Cookson, A. N., Lee, J., Michler, C., Chabiniok, R., Hyde, E., Nordsletten, D. A., ... Smith, N. P. (2012). A novel porous mechanical framework for modelling the interaction between coronary perfusion and myocardial mechanics. *Journal of Biomechanics*, 45(5), 850–855. <https://doi.org/10.1016/j.jbiomech.2011.11.026>
3. Diem, A. K. Valen-Sendstad, K. (2019a) Porous Modelling of Cardiac Perfusion under Contraction to Demonstrate the Distribution of Therapeutic Nanoparticles. *Computing in Cardiology 2019 Proceedings*.
4. Diem, A. K. Valen-Sendstad, K. (2019b) Time-Lapsing Perfusion: Proof of Concept of a Novel Method to Study Drug Delivery in Whole Organs. *Biophysical Journal*, accepted, <https://doi.org/10.1016/j.bpj.2019.09.029>
5. Holzapfel, G. A., & Ogden, R. W. (2009). Constitutive modelling of passive myocardium: A structurally based framework for material characterization. *Philosophical Transactions of the Royal Society A: Mathematical, Physical and Engineering Sciences*, 367(1902), 3445–3475. <https://doi.org/10.1098/rsta.2009.0091>
6. Michler, C., Cookson, A. N., Chabiniok, R., Hyde, E., Lee, J., Sinclair, M., ... Smith, N. P. (2013). A computationally efficient framework for the simulation of cardiac perfusion using a multi-compartment Darcy porous-media flow model. *International Journal for Numerical Methods in Biomedical Engineering*, 29, 217–232. <https://doi.org/10.1002/cnm>